バイオサイエンス研究科　博士論文要旨

| 所属<br>（主指導教員） | Molecular and Cell Genetics (Professor Kenji Kohno) | | |
|---|---|---|---|
| 氏名 | Promlek Thanyarat | 提出 | 平成 23年08月11日 |
| 題目 | The role of unfolded-protein interaction with the stress sensor Ire1 to evoke the endoplasmic reticulum stress response | | |

要旨 **Abstract**

In all eukaryotic cells, impairment of protein folding in the endoplasmic reticulum (ER) leads to ER stress and evokes the unfolded protein response (UPR), which contributes to restoration of conditions in the ER lumen. The UPR is triggered by some transmembrane signal-transducing proteins, among which Ire1 is evolutionally conserved through eukaryotes. Ire1 carries kinase and RNase motifs on its cytosolic domain. Upon ER stress, Ire1 is oligomerized and autophosphorylated for its activation as an RNase. This results in cytoplasmic splicing, maturation in other words, of mRNAs encoding transcription factors, including yeast Hac1, which promote gene induction for the UPR.

To explain the stress-sensing mechanism of Ire1, it is an attractive hypothesis that the luminal domain of Ire1 directly recognizes unfolded proteins accumulated in the ER. According to the X-ray crystal structure of the luminal domain of yeast Ire1, its dimer forms a groove-like structure, which sterically resembles that of the major histocompatibility complex and thus may capture unfolded peptides. Also, a recombinant fragment of the luminal domain of yeast Ire1 was shown to have an ability to interact with unfolded proteins. However, until now, *in vivo* association of Ire1 with unfolded proteins has not been presented.

In this study, a misfolded version of vacuolar carboxypeptidase Y (CPY), CPY*, was employed as an unfolded protein model for demonstrating the interaction of Ire1 with unfolded proteins in yeast cells. Immunofluorescent staining of a GFP-tagged version of CPY* (CPY*-GFP) exhibited that CPY*-GFP cannot reach to the vacuole but is retained in the ER lumen. Also, as expected, cellular expression of CPY*-GFP induced the UPR. Importantly, CPY*-GFP and Ire1 were crosslinked and co-immunoprecipitated from the cell lysates. This complex formation was impaired by the luminal domain mutations mutation points of which are located on or near the groove-like structure, suggesting that CPY*-GFP is directly captured by the groove-like structure.

One of these mutations, the Delta-III mutation, considerably compromised Ire1's ability to evoke the UPR, while Delta-III Ire1 exhibited high-order oligomerization upon ER stress as observed in the wild type.

In the present study, I also generated an experimental technique to check autophosphorylation of Ire1, which includes electrophoresis of protein samples on acrylamide gels containing SDS and $Mn^{2+}$-Phos-tag. By using this method, I noticed that ER stress-dependent phosphorylation of Ire1 is considerably compromised by the Delta-III mutation.

Based on the observations from this study and previous reports, here I propose a scenario for Ire1 sensing of and activation by unfolded proteins accumulated in the ER. Initially, ER stress causes dissociation of an ER-located molecular chaperone BiP from Ire1, which leads to dimerization of Ire1. Through homo-association of the Ire1 dimers, high-order oligomers of Ire1 are formed. Unfolded proteins are then captured by the groove-like structure of the luminal part of the Ire1 dimers, causing a conformational change in the cytosolic part to evoke the cytosolic events, autophsophorylation of Ire1 and activation of its RNase activity.

# The role of unfolded-protein interaction with the stress sensor Ire1 to evoke the endoplasmic reticulum stress response

# 小胞体ストレスセンサーIre1と構造異常蛋白質との会合とその意義

**Thanyarat Promlek**


**Nara Institute of Science and Technology**
**Graduate School of Biological Sciences**
**Molecular and Cell Genetics Laboratory (Professor Kenji Kohno)**
**2011/08/11**

# CONTENTS

# CONTENTS (Continued)

# LIST OF FIGURES

# LIST OF TABLES

# CHAPTER I
# INTRODUCTION

## 1.1 Protein folding in the ER

In eukaryotic cell, secretory and membrane proteins are folded and assembled in the endoplasmic reticulum (ER) before being transported to their target organelles or cell surface via the Golgi apparatus. Protein folding in the ER is facilitated by several ER-resident molecular chaperones and folding enzymes, which recognize various features on the polypeptides. Molecular chaperones bind to nascent polypeptides to prevent their aggregation during the folding process. Protein disulfide isomerase (PDI) shuffles disulfide bonds between cysteine residues, and peptidyl-prolyl *cis-trans* isomerase (PPI) facilitates isomerization of proline residues. Certain molecular chaperones and folding enzymes selectively help folding of proteins carrying N-linked glycosylation.

Protein folding in the ER is operated in cooperating with a quality control mechanism that permits only properly folded proteins to exist the ER to other compartments of the cell. Polypeptides that fail to obtain their native structure are either retained within the ER lumen in complexes with molecular chaperones or directed toward degradation through the 26S proteasome in a process of ER-associated degradation (ERAD).

Protein folding and assembly can be considerably damaged when cells are exposed to various environmental or physiological situations, such as nutrient starvation, calcium depletion from the ER, strong reducing condition, viral infection and hypoxia. Under these conditions, normal protein folding and assembly is likely to be interrupted, leading to accumulation of misfolded and unfolded protein in the ER, namely ER stress. Such situations can also occur upon normal development and differentiation. In response to these harmful conditions, cell activates intracellular signaling pathway termed the unfolded protein response (UPR), which functions to recover normal protein folding capacity in the ER (Hetz and Glimcher, 2009; Ma and Hendershot, 2004; Malhotra and Kaufman, 2007; Ron and Walter, 2007).
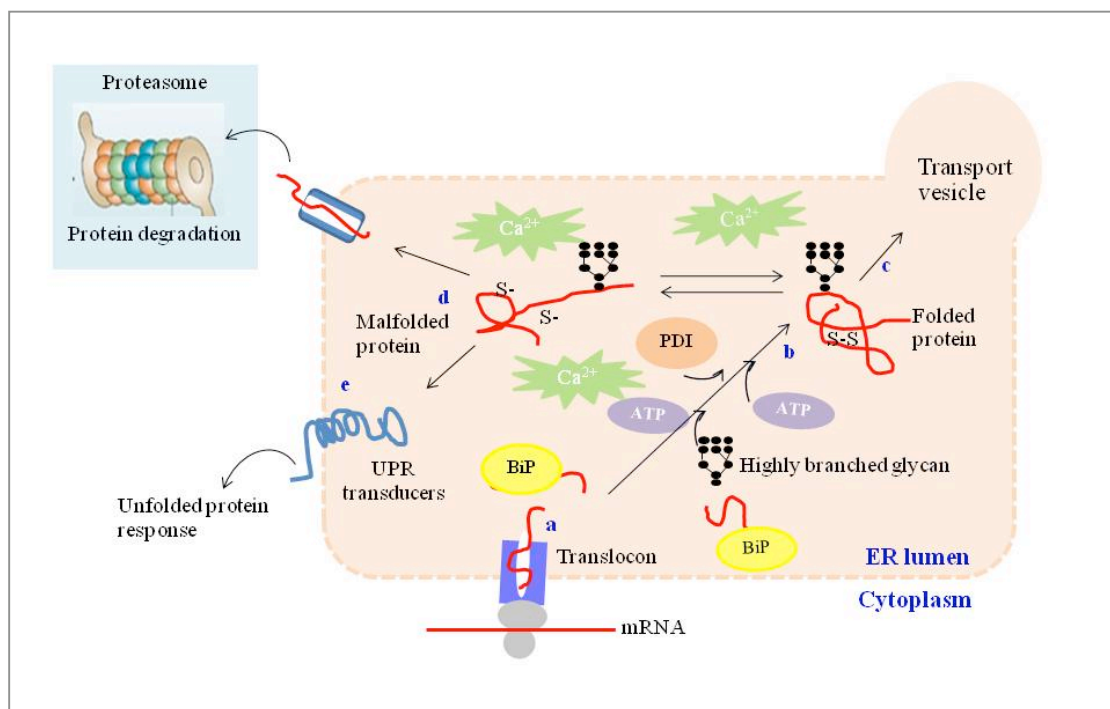
**Figure 1 Protein folding and quality control in the ER.** Process for protein folding in the secretory pathway under normal conditions is shown from a to c. Once ER stress occurs, cells restore the protein folding capacity in the ER by activating mechanisms shown in d and e**.**

**a** | Peptides are translocated into the endoplasmic reticulum (ER) through translocons on the ER membrane. **b** | In the extremely crowded, calcium-rich, oxidizing environment of the ER lumen, ER-resident chaperones such as BiP, calnexin and PDI serve to facilitate proper folding of the nascent peptides. **c** | Once correctly folded and modified, proteins are packed into transport vesicles to exit the ER. **d** | If the ERAD system finds proteins which are malfolded or unable to fold, they are targeted to retrotranslocation to the cytosol and degraded by the proteasome. **e** | When protein folding in the ER is totally impaired, leading to accumulation of unfolded proteins in the ER, three ER-stress sensors — IRE1, PKR-like ER kinase (PERK) and ATF6 — initiate the UPR**.**

## 1.2 The unfolded protein response pathway (UPR)

The UPR pathway, which is a conserved signaling pathway in all eukaryotic cells, controls and adjusts ER homeostasis and capacity of protein folding and secretion. The main role of the UPR is transcriptional induction of factors for protein folding, such as molecular chaperones, PDI and PPI and for the ERAD. In addition, the UPR includes global translational attenuation in metazoan cells, probably in order to decrease protein loading into the ER (Bernales et al., 2006; Ron and Walter, 2007).

To date, three different classes of ER stress sensors, Ire1, ATF6 (Activating transcription factor-6) and PERK (PKR-like ER kinase), have been identified on the ER of metazoan cells. Among them, only Ire1 is evolutionarily conserved through eukaryotes (Cox et al., 1993; Harding et al., 2000; Sidrauski and Walter, 1997; Yoshida et al., 1998).

## 1.3 IRE1: the conserved core of the UPR

Ire1 is an ER stress sensor which was initially identified through a genetic screen for mutations that block the UPR in yeast cells (Mori et al., 1996). The *IRE1* gene encodes a type I ER-resident transmembrane protein with a luminal domain, which has known functional motif, and a cytoplasmic portion that contains a protein kinase and a site specific endoribonuclease (RNase) motifs (Fig. 2) (Cox et al., 1993; Tirasophon et al., 1998). In response to accumulation of unfolded protein in the ER, Ire1 oligomerizes on the ER membrane and performs trans-autophosphorylation, which leads to its activation as an RNase (Shamu and Walter, 1996; Tirasophon et al., 2000). The most well-known substrates of Ire1 are mRNAs that encode transcription factors Hac1 (Homologous to ATF and Cre binding protein) in yeast (Cox and Walter, 1996; Kawahara et al., 1997; Mori et al., 1996) and XBP1 (X-box binding protein-1) in metazoans (Calfon et al., 2002; Yoshida et al., 2006).

Ire1 cleaves the precursor form *HAC1* or XBP1 mRNA (*HAC1*$^u$/XBP1$^u$) at two positions for excising of the intron. The 5' and 3' exon fragments are then ligated, generating a spliced mRNA (*HAC1*$^i$/XBP1$^s$), which is translated to a transcriptional
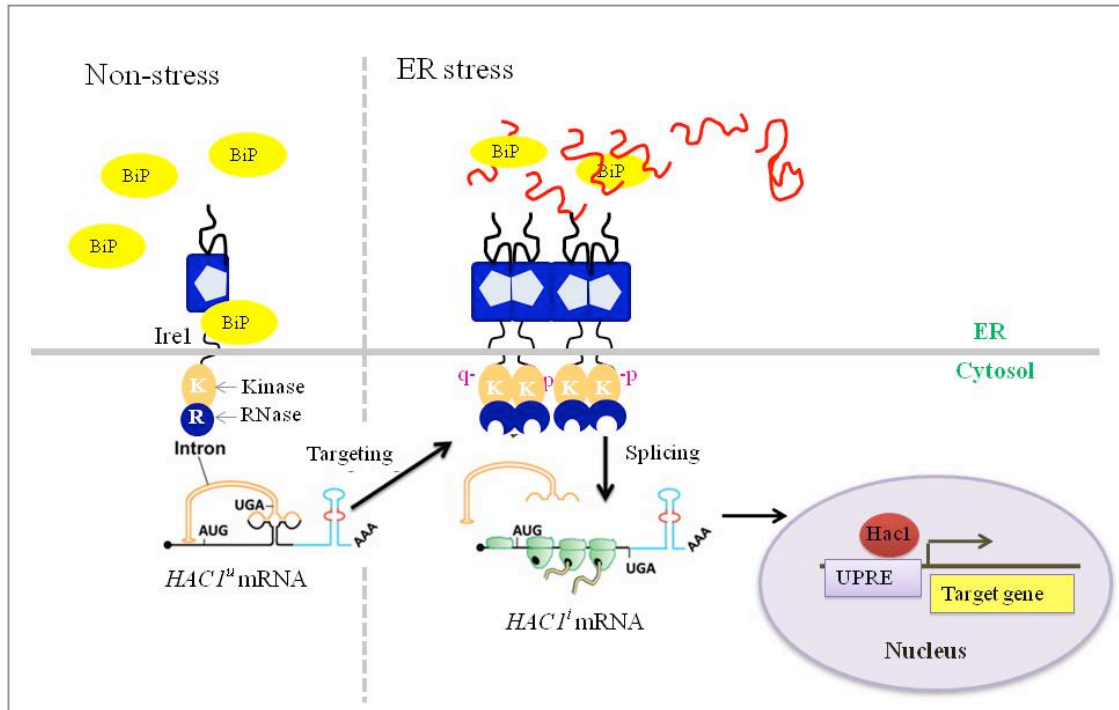
**Figure 2 Ire1 signaling pathway in yeast cells.** Under ER stress condition, untranslated $HAC1^u$ mRNA, whose translation is attenuated by hybridization of its intron with its 5'UTR, is recruited to Ire1 cluster dependently on its 3'UTR sequence (red color). Activated Ire1 excises the intron out and generates $HAC1^i$ mRNA, which can be translated to the active Hac1 transcription factor. Hac1 moves to nucleus to induce transcription of UPR target genes.

activator protein for the UPR target genes. In yeast, the enzyme that is responsible for the ligation reaction is Rlg1, which is a tRNA ligase (Sidrauski et al., 1996; Sidrauski and Walter, 1997), while in metazoan, the ligation enzyme has not yet been identified. The translational products of these mRNAs, Hac1 and XBP1 proteins, move into the nuclei and induce gene expression as aforementioned. For induction of certain UPR target genes, such as those encoding BiP and PDI, Hac1 and XBP1 proteins interact with the gene promoters carrying the Unfolded protein response element (UPRE) (Cox and Walter, 1996; Mori et al., 2000) in yeast or the ER stress response element (ERSE) in mammalian cells (Yoshida et al., 1998).

**1.4 Stress sensing mechanism by Ire1**

The N-terminus moiety of Ire1 resides in the ER lumen is believed to act as a sensor to monitor the ER stress status. The signal then has to be transmitted across the ER membrane to activate the kinase and RNase domains. ER chaperone protein BiP has been proposed to be a negative regulator of Ire1. According to Bertolotti et al. (2000) and Okamura et al. (2000) BiP is associated with the luminal domain of Ire1 to inactivate Ire1 under non-stress conditions. Upon ER stress, BiP dissociates from Ire1. Unfolded proteins accumulated in the ER may competitively dissociate BiP from Ire1. Meanwhile, it should be noted that the BiP dissociation form Ire1 is not sufficient for full activation of Ire1 as an RNase at least in yeast cells, since as described below, an Ire1 mutant lacking the BiP-binding segment is still upregulated by ER stress.

Kimata et al. (2004) and Credle et al. (2005) precisely analyzed the structure of the luminal domain of yeast Ire1. According to these reports, the luminal domain can be segmented into five subregions (I-V) from the N-terminal to the jaxtamembrane position (Fig 3A). Subregions II and IV form a tightly folded domain, namely the core of the luminal domain (cLD), while Subregions I and V are loosely folded. Subregion III is likely to be a flexible loop sticking out form cLD.

The BiP-binding site has been assigned on subregion V, since Delta-V mutant Ire1, in which subregion V was deleted, showed almost no association with BiP even under non-stress conditions. A molecular event(s) independent of the BiP dissociation

is required for full activation of Ire1, since Delta-V Ire1 was regulated by ER stress as well as wild-type Ire1 (Kimata et al., 2007; Kimata et al., 2004; Oikawa et al., 2007; Oikawa et al., 2005).

According to the X-ray crystal structure of the yeast cLD reported by Credle et al. (2005), it has two different homo-association interfaces, namely interfaces I and II. This suggests that Ire1 forms oligomer as illusustrated in Fig. 3B. Consistently, microscopic observation of cellular localization of Ire1 indicates that Ire1 is highly oligomerized on the ER membrane upon ER stress. It is likely that binding of BiP to subregion V suppresses the oligomerization of Ire1, while it is also somehow inhibited by subregion I under non-stress conditions, since Delta-I (deletion of subregion I) Delta-V double deletion mutant Ire1, but not Delta-I or Delta-V single mutant, clustered constitutively even without ER stress. It should be noted that the oligomerization is not sufficient for activation of Ire1. Delta-I Delta-V Ire1 was still regulated in an ER stress-dependent manner.

Another important insight from the X-ray crystal structure of the yeast cLD is that it forms a groove-like structure, which sterically resembles that of the major histocompatibility complex (MHC), when dimerized via interface I (Fig. 3C). This leads to a speculation that unfolded peptides or misfolded proteins might be captured by the groove. Supporting this idea, a recombinant fragment of the cLD prevented aggregation of denatured proteins *in vitro*.

Kimata et al. thus proposed a hypothetical scenario by which Ire1 is activated upon ER stress (Fig 4). First, BiP dissociates from Ire1, resulting oligomerization of Ire1. Second, direct association of unfolded proteins with Ire1 oligomer somehow leads to full activation of Ire1.
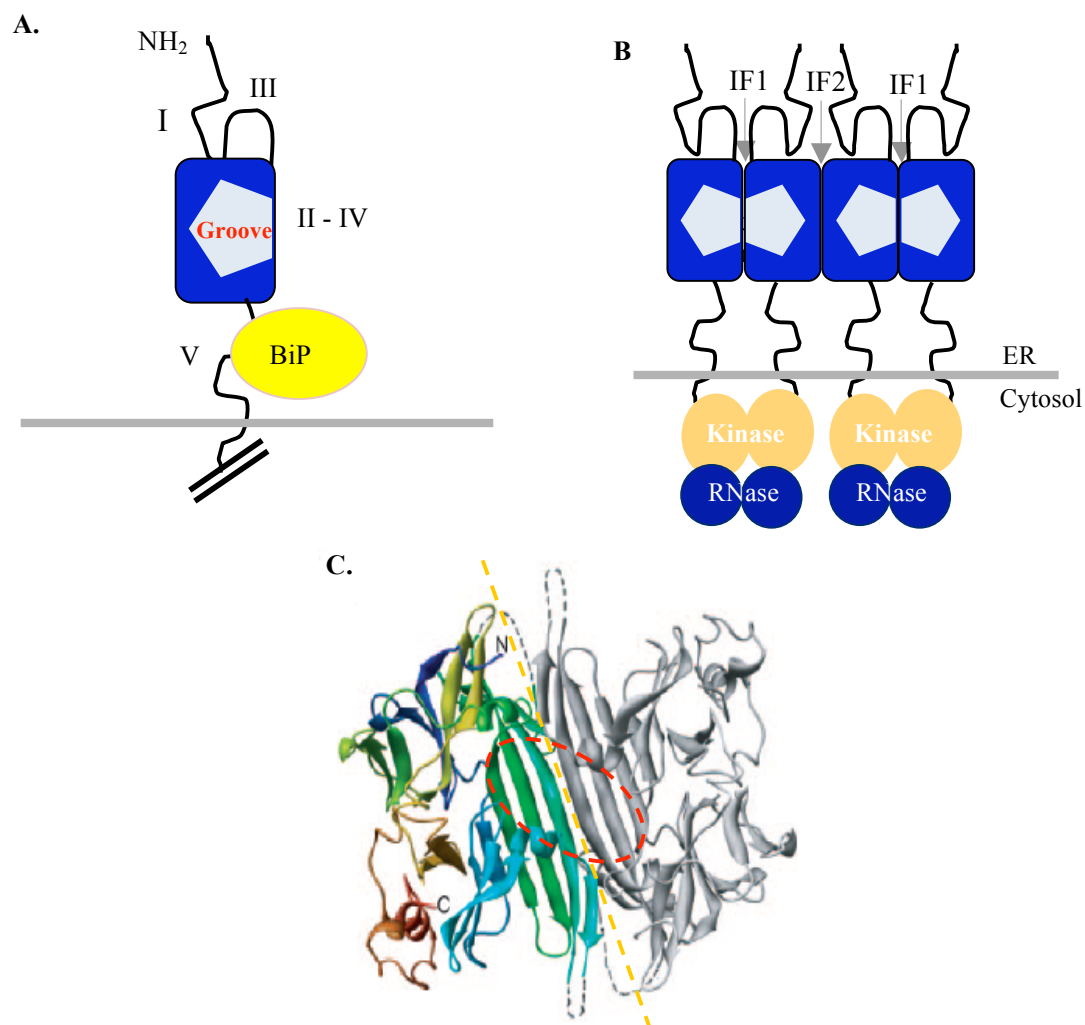
**Figure 3 Structure of yeast Ire1.** (**A**) Structure of the yeast luminal domain is proposed by Kimata et al. (2007). It is divided into five subregions. The cLD is composed of subregion II, III and IV. Subregions II and IV form a tightly folded domain, while subregion III is a loosely folded segment. BiP associates with subregion V.

(B) **High-order oligomerization of Ire1** by homo-association *via* Interfaces I (IF1) and II (IF2)

(C) **The X-ray crystal structure of the cLD dimer homo-associated via interface I (the orange broken line).** The red broken-line circle shows the location of the groove-like structure.

**Figure 4 A hypothetical model explaining two-step activation of Ire1 upon ER stress.** See text for detail.
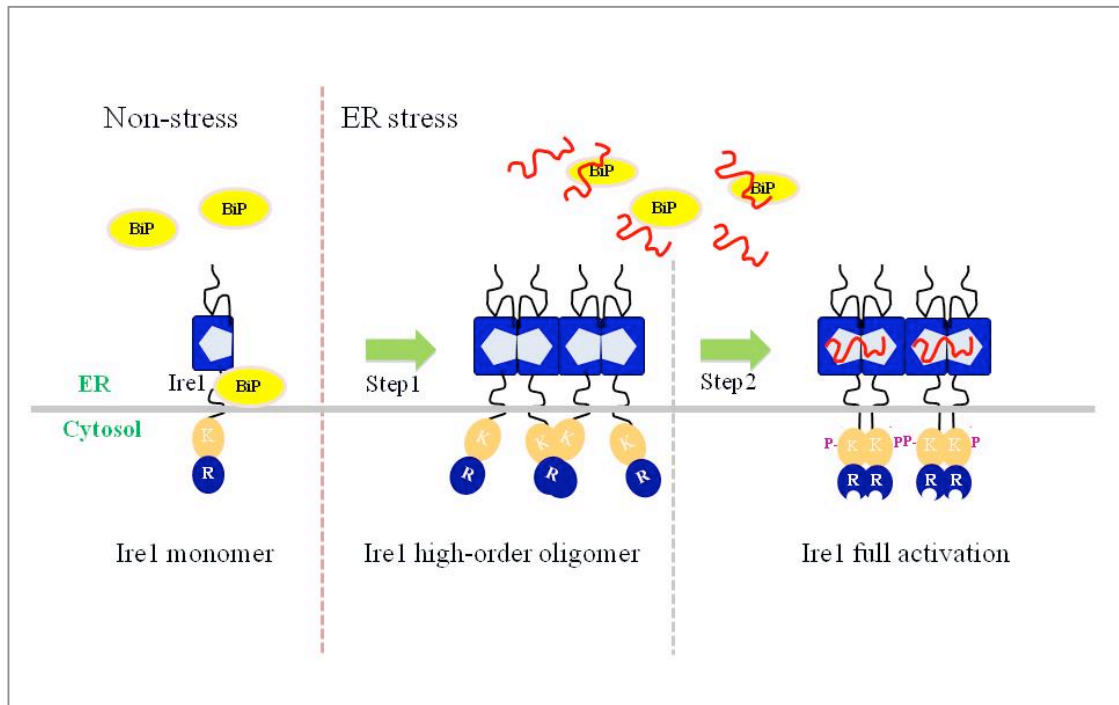
In the present study, I generated an easy-to-detect model of ER-accumulating unfolded proteins, using CPY*-GFP. By expressing this protein in yeast cells, I demonstrated that Ire1 is associated with unfolded proteins in yeast cells. Mutational study of Ire1 strongly suggests that as expected, the groove-like structure on cLD plays a significant role in formation of this complex. As aforementioned, activation of Ire1 as an RNase accompanies its oligomer formation and autophosphorylation. Finally, we thus approached a causal relationship between these molecular events and the unfolded protein-Ire1 association, in order to figure out molecular steps by witch Ire1 is activated upon accumulation of unfolded proteins in the ER.

# CHAPTER II
# MATERIALS AND METHODS

## 2.1 Plasmid constructions

### 2.1.1 Expression plasmid for CPY-GFP and CPY*-GFP

To construct plasmid for expression of CPY-GFP and CPY*-GFP under the control of the *TEF1* or *GAL1* promoter, DNA fragments were obtained by using PCR primers listed in Table 1. DNA fragments corresponding to the *TEF1* and the *GAL1* promoters and the CPY-coding sequence were amplified from genomic DNA of yeast, while the coding sequences for CPY* and yeast enhanced GFP (EGFP) were amplified respectively from pRS306-prc1-1 (Finger et al., 1993; Kohno Lab) and pKT209 (Humpolickova et al., 2009). The PCR product of the *TEF1* or *GAL1* promoter was inserted into pRS313 yeast *HIS3* centromeric vector at the *Not*I and *Spe*I site, resulting in pRS313-TEF1 or pRS313-GAL1. The DNA fragment encoding either CPY or CPY* was ligated with EGFP at *Eco*RI site and then cloned into pRS313-TEF1 and pRS313-GAL1 at the *Spe*I and *Xho*I sites (Fig. 5).

### 2.1.2 Expression plasmid for mutant versions of Ire1-HA

To create mutations on the luminal domain of *IRE1*, partial fragments of *IRE1* carrying the mutations were amplified from pRS315-IRE1-HA (Kimata et al., 2003; Kimata et al., 2004; Okamura et al., 2000) by using the overlap PCR technique with primers P1, P2 and internal mutagenic primers which are listed in Table 2. The *IRE1* mutant fragments were joined into plasmids by using the *in vivo* homologous recombinant (gap repair) technique as described in Kimata et al. (2004). The resulting plasmids were extracted from yeast cells for confirming their sequence. Furthermore, HA-tagged Ire1 (Ire1-HA) gene fragments containing the indicated mutations were existed from the mutant versions of pRS315-IRE1-HA by digestion with *Bam*HI and *Not*I and cloned in to a yeast 2μ *URA3* vector pRS426 at the same restriction sites.
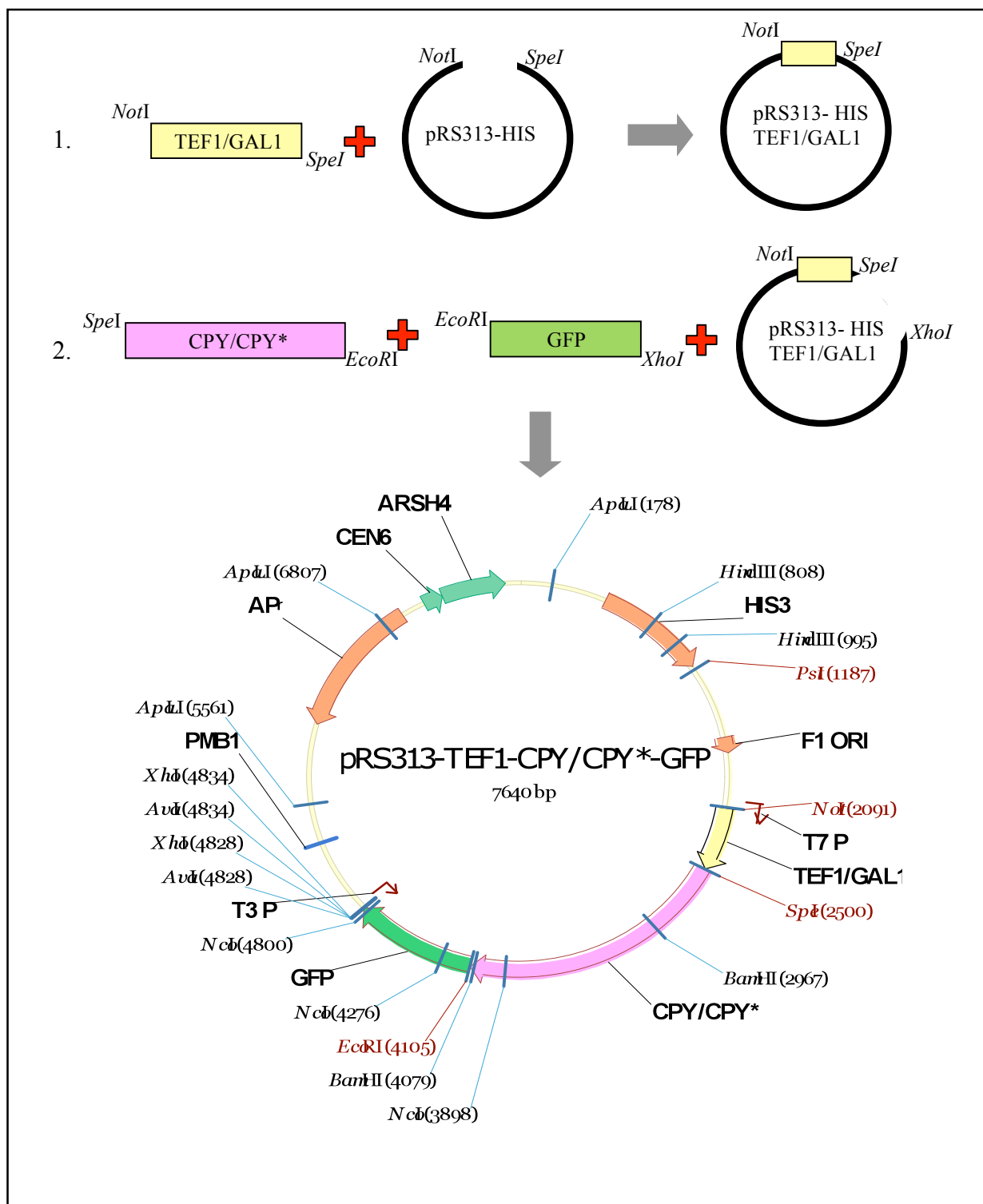
**Figure 5 Scheme for constructing expression plasmids for CPY-GFP or CPY*-GFP**.

**Table 1 PCR primer 1**

| Target | Primer name | Primer sequence |
|---|---|---|
| *TEF1* promoter | f'Not-1 TEF1 | ATATATATGcggccgcATAGCTTCAAAATGTTTCTACTCC |
| | r'speI-TEF1 | ATATATactagtAAACTTAGATTAGATTGCTATGCT |
| *GAL1*promoter | f'Not-1pGAL1 | ATATATgcggccgcACGGATTAGAAGCCGCCGAGC |
| | r'speI- pGAL1 | ATATactagtGGTTTTTTCTCCTTGACGTTAAAGTATAGAGG |
| CPY/CPY* | f' speI-CPY | GTTTAactagtAAATGAAAGCATTCACCAGTTTACTATGTGG |
| | r'EcoRI-CPY | TTTAAgaattcTAAGGAGAAACCACCGTGGATCCAT |
| GFP | Sense GFP -EcoRI | GGTTTAgaattcAAAGGTGAAGAATTATTCACTGGTGTTG |
| | antisense GFP XhoI | TTAAActcgagTTATTTGTACAATTCATCCATACCATG |
| *HAC1* | f' HAC1 | TACAGGGATTTCCAGAGCACG |
| | r'HAC1 | TGAAGTGATGAAGAAATCATTCAATTC |

Small letters indicate the recognition sites of restriction enzymes.

**Table 2 PCR primer 2**

| Primer type | Name | Mutation | Primer sequences |
|---|---|---|---|
| Internal mutation primers | Groove mutant | M229A | GAAAAGGTCTACACTGGATCGGCAAGAACTATAATGTATACTATAAAC |
| | | F285A | ATGATTGTAATAGGCAAAACTATTGCTGAGCTGGGAATTCACTCTTAT |
| | | Y301A | GGAGCAAGCTACAATGTCACTGCCTCTACATGGCAGCAAAATGTT |
| | IF1 | T226W | TGAAAAGGTCTACTGGGGATCGATGAG |
| | | F247A | TGAATGGTGAAATTATATCAGCAGCAGGACCTGGTTCAAAAAACGGGTAT |
| | IF2 | W426A | AGATACGCTTCCAGTGACCGTGCAAGGGTGTCTTCAATTTTTGAAGAT |
| | Delta-III | Deletion of subregion III | CAGCGTTCGGACCTGGTTCAAAAGAATCTGAAAATATGATTGTAATAGGC |
| Reverse primers that are exactly complementary to the forward internal mutation primers were also used. | | | |
| External primers | P-1 (Forward primer) | | CCATTATCACTTTTCTCCATATCA |
| | P-2 (Reverse primer) | | CCTTGAAAACTTCCCTGAAAAACT |

## 2.2 Yeast stain and growth conditions

Yeast haploid strain KMY1015 (*MATα ura3-52 leu2-3,112 his3-Δ200 trp1-Δ900 lys2-801 Δire::TRP1*) provided by K. Mori (Kyto University, Kyoto, Japan) was used as the original source in this study. Cells were grown in minimal synthetic dextrose (SD) medium (2% glucose and 0.66% yeast nitrogen base without amino acids; Difco) supplemented with appropriate amino acids. The *GAL1* promoter was induced by preculturing cells in 2% raffinose medium (2% raffinose and 0.66% yeast nitrogen base without amino acids; Difco) for 2 h followed by addition of 2% galactose. All incubations were performed at 30°C.

## 2.3 Yeast transformation

Cells were precultured overnight in 1 ml of yeast peptone dextrose (YPD) medium before transferring to 50 ml YPD medium in 300 ml flask and further incubated at 30°C until mid-log phase. Cultured cells were collected by centrifugation at 3,000 rpm for 1 min. Cells were then washed with 10 ml of 0.1 M LiAc solution and suspended with 1 ml of this solution. Suspended cells were incubated at 30°C for 1 h with 60 rpm shaking. Then 100 μl of the cells suspension was added into a tube containing 5 μl of carrier DNA and 1 μg of transforming DNA. The transformation mixture was incubated at 30°C for 30 min. Then 800 μl of 40% PEG 4000 in 0.1 M LiAc was added into the transformation mixture, which was further incubated at 30°C for 2 h. Finally, cells were plated onto a selection plate and further incubated for 3 day.

## 2.4 Immunofluorescent staining

Cells were fixed in 0.1 M postassium acetate buffer, pH 6.8 containing 3.3% formaldehyde for 2 h and processed essentially as described in Kimata et al. (2007). The antibodies used here are listed in Table 3. The specimens were mounted with vectashield® mounting medium with DAPI and viewed under a fluorescent microscope (Carl Zeiss Axophoto).

**2.5 Reverse transcription (RT)-PCR assay to check *HAC1* mRNA splicing**

Total RNA samples were prepared by using hot phenol method as described in Kimata et al., 2004. 1 μg of total RNA sample was used to generate cDNA by using the Superscript™II Reverse Transcriptase (Invitrogen) and oligo (dT) primers according to the manufacturer's protocol. *HAC1*$^u$ and *HAC1*$^i$ products were PCR amplified by using primers flanking the intron (Table 1) with the thermocycle condition 95$^o$C, 5min; 25 cycles of (94$^o$C, 1min; 54$^o$C, 0.30 min; 72$^o$C, 1 min) and 72$^o$C, 7min. The PCR products were fractionated by electrophoresis on 1.5% agarose gel.

**2.6 β-galactosidase assay**

Cells grown to log phase were collected and suspended in 800 ul of Z-buffer (60 mM $Na_2HPO_4$, 40 mM $NaH_2PO_4$, 10 mM KCl, 1mM $MgSO_4$, 0.27% 2-mercaptoethanol, pH 7.0). After adding of 20 μl of 0.1% SDS and 50 μl of chloroform, the mixture was vigorously mixed for 20 second and equilibrated to 28$^o$C. The substrate, o-Nitrophennyl-D-galactoside (4 mg/ml in Z-buffer) was then added to a final concentration 0.8 mg/ml and further incubated at 28$^o$C for duration until the mixture showed a pale yellow color. The reaction was terminated by adding 0.5 ml of 1 M $Na_2CO_3$. The concentration of product, o-nitrophenol (ONP), was measured at $A_{420}$. One unit of β-galactosidase activity is defined as 1nmol ONP production per minute of reaction per ml of yeast culture at 1 $OD_{600}$. The β-galactosidase activity was calculated by this formula.

$$\beta\text{-galactosidase activity} = \frac{OD_{420} \times 375}{(OD_{600}) \times \text{time (min)}}$$

**2.7 Chemical crosslinking co-immunoprecipitation**

The detail and dilution of used antibodies in immunoprecipitation and Western blot analyses are shown in Table 3.

25 $OD_{600}$ equivalent cells were suspended in 800 μl of PBS buffer and incubated with 2 mM dithiobis (succinimidyl) propionate (DSP; freshly prepared in DMSO at 200 mM) at room temperature for 1 h. The crosslinking reaction was quenched by addition of 100 mM of Tris (pH 7.5) and further incubation at room temperature for 30 min.

Total protein samples were prepared under non-denaturing condition as described Kimata et al. (2003). In brief, cells were disrupted by glass beads in 200 μl of 1% Tritron-X lysis buffer containing protease inhibitors (1 mM PMSF, 0.2 mg/ml leupeptin, apotinin and pepstatin A). The cell lysates were clarified by centrifugation at 13,000 rpm for 10 min.

To perform immunoprecipitation, 150 μl of cell lysates were diluted in 850 μl of 6% skim milk in IP buffer (60 mM Tris-HCl pH 7.9, 6 mM EDTA, 180 mM NaCl, 1% Triton X-100) and pre-cleared with 30 μl of 50% protein-A-conjugate Sepharose beads (protein-A-Sepharose 4FF; Amersham Biosciences) for 1 h at 4°C, supernatant was incubated with 2 μl of anti-GFP antibody or 5 μl of anti-HA antibody at 4°C for 6 h. The reactions were centrifuged 13000 rpm at 4°C for 10 min. The clear solution was collected and followed by the addition of 30 μl of 50% protein A-conjugated Sepharose beads. After further incubation at 4°C for 1 h, the Sepharose beads were collected by centrifugation, washed 5 times with washed buffer (50 mM Tris-HCl pH 7.9, 5 mM EDTA, 150 mM NaCl, 1% Triton X-100). The immunoprecipitants were analyzed by anti-HA and anti-GFP Western blot analysis.

**2.8 Western blot analysis**

The lysates and immunoprecipitates were denatured in SDS/DTT-sampling buffer and reveal on 8% SDS-PAGE. The protein in the gel was electrophoretically transferred onto immobilon-P transfer membrane (Millipore) by semi-dry blotting at 1 $mA/cm^2$ for 2 h. The transfer membrane was blocked in blocking buffer containing 3% BSA in 0.2%

PBST for 1 h before probing with anti-HA or anti-GFP at RT for 1.30 h and then washed 3 times with 0.2% PBST, 10 min in each time. The blocking buffer containing HRP-coupled secondary antibody was incubated with the membrane at RT for 1 h. After 3 times washing with 0.2% PBST, the membrane was developed by ECL system (Amersham Biosciences). ECL signal was detected by X-ray film exposure.

### 2.9 Phos-tag-gel

Phos-tag gel was carried out the same way as regular western blots, except that: (a) the protein sample was prepared in present of phosphatase inhibitor cocktail (Roche) and without EDTA (b) 5% SDS-PAGE containing 25 $\mu$M Phos-tag (NARD Institute) and 25 $\mu$M $MnCl_2$ (Sigma) were used; (c) gels were soaked in 1 mM EDTA for 10 min before transfer onto a immobilon-P transfer membrane (Millipore).

**Table 3 List of antibody**

| Detection | 1st Antibody | Company | Dilution | 2nd Antibody | Company | Dilution |
|---|---|---|---|---|---|---|
| **Immunofluorescence staining** | | | | | | |
| CPY-GFP/CPY*-GFP | Chicken polyclonal antibody to GFP IgY fraction | Aves | 1:100 | FITC conjugated donkey anti-chicken IgY | Jackson Immunoresearch Labaratory | 1:50 |
| BiP | Rabbit polyclonal antibody to BiP | Tokunaga et al., 1992 | 1:1000 | $Cy^{Tm}$ 3 conjugated anti-rabbit IgG | ,, | 1:200 |
| **Western blot analysis** | | | | | | |
| CPY-GFP/CPY*-GFP | Rabbit polyclonal antibody to GFP | Medical& Biological Laboratory (MBL) | 1:1000 | HRP-conjugated donkey anti-rabbit IgG | ,, | 1:8000 |
| Ire1-HA | Mouse monoclonal antibody clone 12CA5 to peptide epitope HA | Kohno Lab | 1:2500 | HRP-conjugated goat anti-mouse IgG | ,, | 1:8000 |

# CHAPTER III

# RESULTS

## 3.1 CPY*-GFP acts as an ER-retained model unfolded protein

In order to demonstrate interaction of Ire1 with unfolded proteins, I used the well-characterized misfolded mutant of carboxypeptidase Y (CPY), CPY* (Finger et al., 1993; Spear and Ng, 2003), as a model unfolded protein. Wild-type CPY is synthesized as an inactive preproenzyme, which traverses through the ER, the Golgi apparatus and the vacuole as the final destination. Since the signal peptide of preproCPY is digested upon its translocation into the ER. In the oxidizing lumen envelopment, five intrachain disulfide bonds and four N-linked glycans are added to produce proCPY (Fig. 6). Then a vacuolar peptidase removes the pro segment of proCPY for its conversion to the mature form (mCPY) in vacuole (Jung et al., 1999). CPY*, the mutated protein carries the amino acid substitution G255 to R (Finger et al., 1993), two positions before the active-site, a region highly conserved in all serine protease. CPY* is completely devoid of catalytic activity. In contrast to wild type pro-CPY which can be matured by trypsin yielding active CPY, CPY* exhibits a high sensitivity toward trypsin digestion in vitro. Thus the tertiary structure of CPY* is assumed as a misfolded protein.

Here, I constructed fusion genes for wild-type CPY and CPY* carrying C-terminal GFP tag (CPY-GFP and CPY*-GFP), expression of which were driven by the constitutive TEF-1 promoter. Expression of the proteins was detected by anti-GFP Western blot analysis of cell lysates. Wild-type CPY-GFP appeared as double protein bands, while CPY*-GFP appeared only as a low-mobility band (Fig. 7). Cleavage of the pro segment in the vacuole is known to decrease the molecular weight of CPY (Jung et al., 1999). Also considering cellular localization of wild-type CPY-GFP and CPY*-GFP (Fig. 8), which is detailed in the next paragraph, I assign two protein bands of wild-type CPY-GFP as the ER-located pro form (proCPY-GFP) and the vacuole-located mature form (mCPY-GFP), while CPY*-GFP seemed to mostly exist
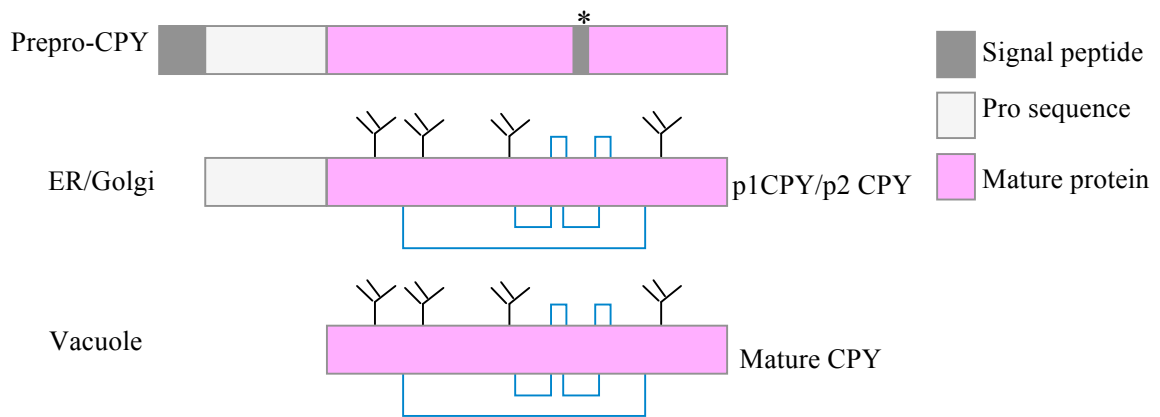
**Figure 6 Schematic representation of CPY**. After translocation in the ER, the signal sequence is cleaved, N-glycans are attached and disulfide bonds are formed. Sugars are modified in the Golgi from where the protein is sorted to the vacuole. Here the pro-region is removed and the enzyme becomes active. The asterisk indicates the point mutation G255 to R present in CPY*. Y: N-link glycan, ⊓ : disulfide bond.
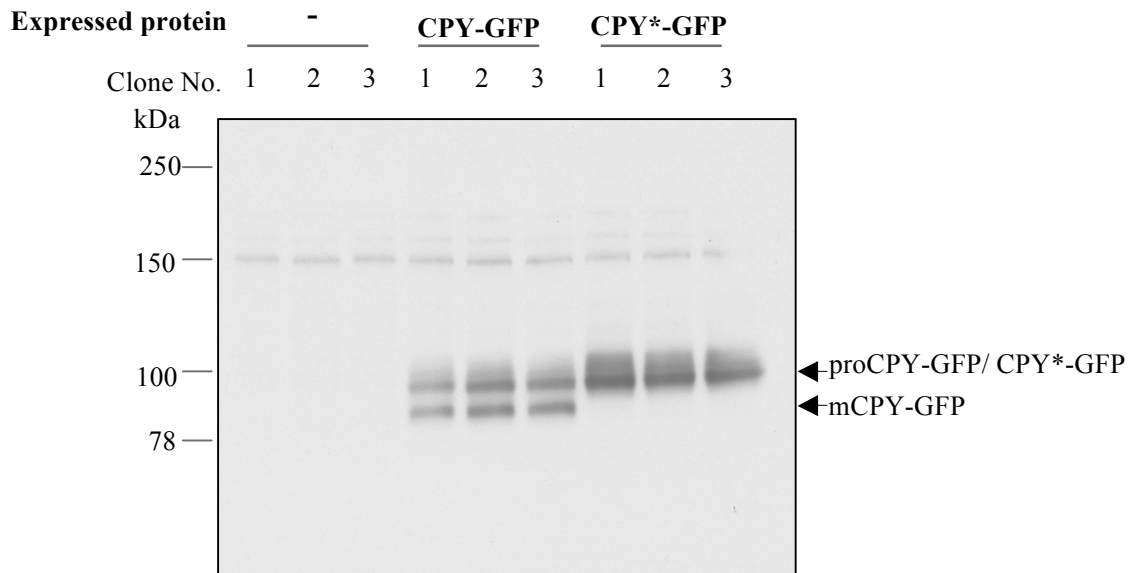
**Figure 7 Expression of CPY-GFP or CPY\*-GFP.** KMY1015 (*ire1Δ*) yeast strain carrying pRS315-IRE1-HA (for expression of HA-epitope tagged Ire1 (Ire1-HA)) were transformed with pRS313-CPY-GFP, pRS313-CPY\*-GFP (for expression of CPY-GFP or CPY\*-GFP) or empty vector of pRS313. Cell lysates were run on 8% SDS-PAGE. The resulting gel was then analyzed by immunoblotting with anti-GFP antibody.  Three independent transformants (clone No. 1 to 3 for each expression plasmid) were checked.

as the ER-retained pro form. This is consistent with the case of non-tagged CPY and CPY* (Finger et al., 1993).

In order to determine subcellular localization of wild-type CPY-GFP and CPY*-GFP, I performed double immunofluorescent staining by using anti-GFP antibody together with anti-BiP antibody. The fluorescent staining pattern of CPY*-GFP overlapped with that of the ER which is visualized by co-staining with anti-BiP antibody (Fig. 8), indicating that CPY*-GFP is retained in the ER lumen. As expected, the staining signal of wild-type CPY-GFP did not completely merge with the ER marker. This result again claims that wild-type CPY-GFP is transported out from the ER to the vacuole, whereas CPY*-GFP cannot pass the quality control system in the ER.

I next determined activation of the UPR pathway in cells expressing wild-type CPY-GFP or CPY*-GFP through checking the *HAC1* mRNA splicing together with monitoring expression of the β-galactosidase reporter gene (*lacZ*) driven by the UPRE (Kohno et al., 1993; Mori et al., 1992). Both strategies showed that the UPR was activated even by expression of wild-type CPY-GFP. However, as expected, CPY*-GFP had much stronger ability to activate the UPR (Fig. 9).

Taken together, CPY*-GFP is retained in the ER as an unfolded protein which strongly activates the UPR pathway. It is also likely that wild-type CPY-GFP somewhat unfolded, although not obviously. Thus, I employed CPY*-GFP as a model of unfolded protein to investigate mechanism of Ire1 activation by unfolded proteins.
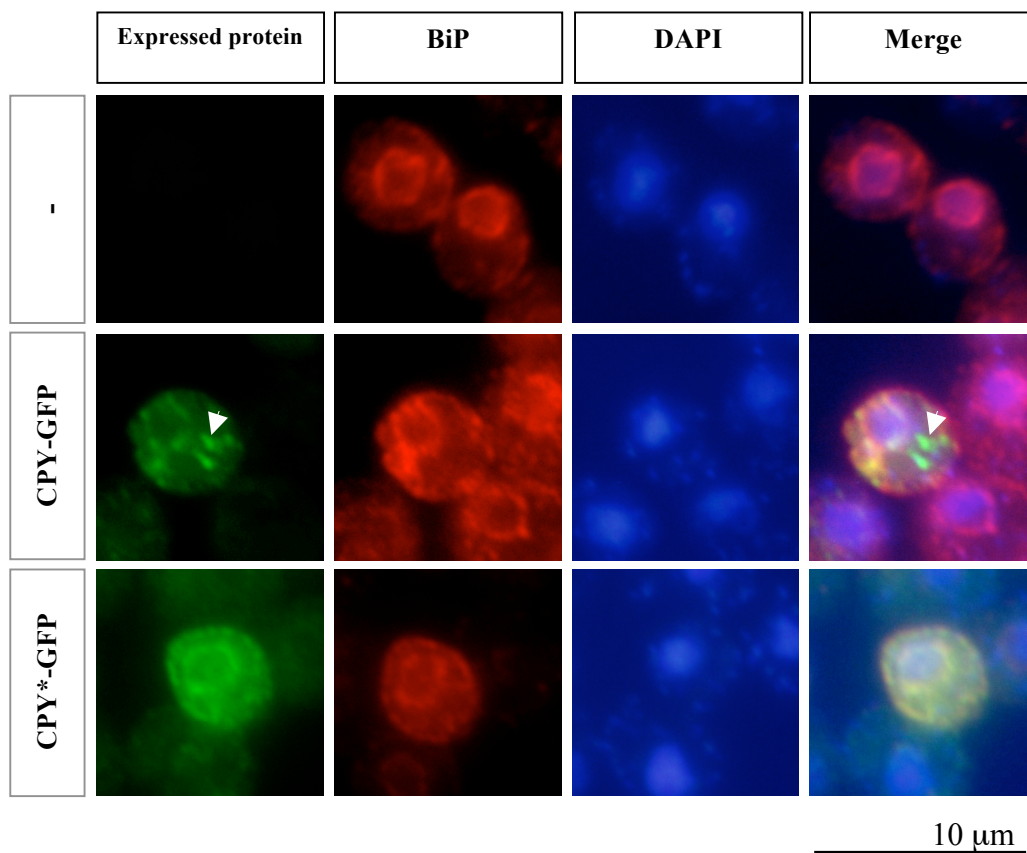
|  | Expressed protein | BiP | DAPI | Merge |
|---|---|---|---|---|
| - | | | | |
| CPY-GFP | | | | |
| CPY*-GFP | | | | |

10 μm

**Figure 8 Localization of CPY-GFP and CPY\*-GFP**. Cells employed in Fig. 7 were probed with chicken anti-GFP (green; FITC) and rabbit anti-BiP (red; Cy3). The white arrow indicates a signal of CPY-GFP transported out from the ER.
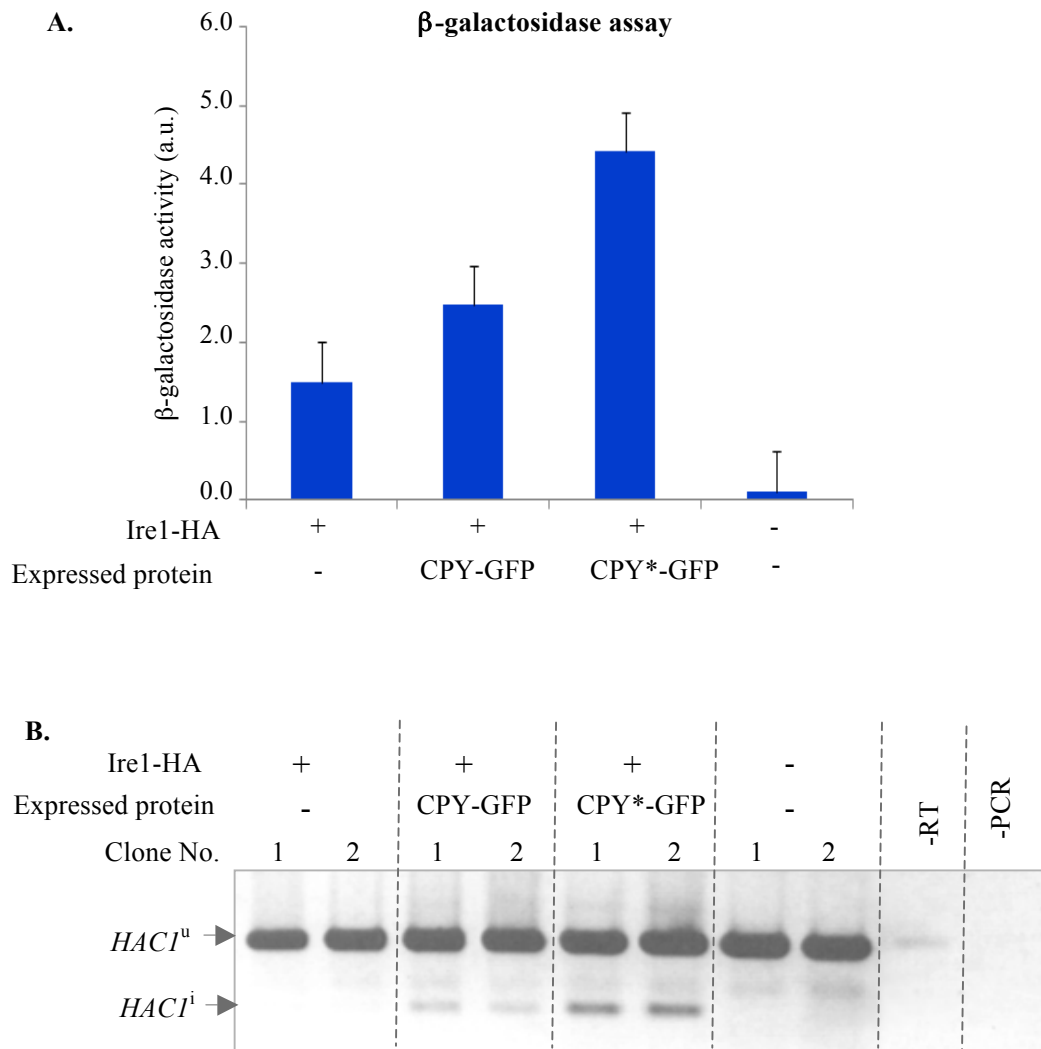
**A.**



**B.**



**Figure 9 Activation of UPR in cell expressing CPY-GFP or CPY\*-GFP**. pRS313-CPY-GFP, pRS313-CPY\*-GFP or empty vector of pRS313 were introduced into KMY1015 (*ire1Δ*) cells carrying the UPRE-*LacZ* reporter gene and pRS315-IRE1-HA. Cells were then subjected to β-galactosidase assay (**A**) or *HAC1* mRNA splicing assay (**B**). In (**B**), total RNA samples were subjected to RT-PCR to amplify spliced *HAC1* (*HAC1$^i$*) and unspliced *HAC1* (*HAC1$^u$*). Two individual clones (Clone No. 1 and 2) were used for parallel experiments.

## 3.2 Ire1 associates with the model unfolded protein

As described in the Introduction section, the X-ray crystal structure of the luminal domain of yeast Ire1 reveals that upon dimerization, it forms a groove-like structure that resembles the peptide-binding structure of MHC (Credle et al., 2005). Also, Kimata et al. (2007) demonstrated that a recombinant protein of yeast Ire1 luminal domain prevents aggregation of denatured proteins *in vitro*, suggesting unfolded protein-associating ability of this protein. In order to confirm that unfolded proteins are actually associated with the Ire1 luminal domain *in vivo*, I performed co-immunoprecipitation assay (Fig. 10A). The *IRE1* knockout cells carrying a 2μ plasmid for expression of Ire1-HA were transformed with the expression plasmid for CPY-GFP or CPY*-GFP. Before lysed, cells were treated with dithiobis succinimidyl propionate (DSP), the membrane-permeable crosslinker. Total protein samples were then immunoprecipitated with anti-GFP antibody. The following Western blot analysis with anti GFP antibody showed that CPY*-GFP were well immunoprecipitated as well as mature and proCPY-GFP. Importantly, anti-HA Western blot analysis of the anti-GFP immunoprecipitates showed co-immunoprecipitation of Ire1-HA with CPY*-GFP. No Ire1-HA signal was detected from the anti-GFP immunoprecipitate from cells expressing neither wild-type CPY-GFP nor CPY*-GFP.

It also should be noted that although weakly, wild-type CPY-GFP co-immunoprecipitated Ire1-HA (Fig. 10A). One possible explanation for this finding is that folding of proCPY-GFP is somewhat impaired, so that it is partially trapped by the quality control system in the ER (Fig. 8). This idea is supported by slight evocation of the UPR by expression of wild-type CPY-GFP (Fig 9).

*In vivo* interaction between Ire1-HA and CPY-GFP or CPY*-GFP were confirmed by a reverse immunoprecipitation experiment, which showed that both CPY*-GFP and the pro form of wild-type CPY-GFP were co-immunoprecipitated with Ire1-HA (Fig. 10B). Importantly, mCPY-GFP was not observed in the co-immunoprecipitation samples, indicating that as expected, the protein interaction occurs in the ER. As well as the case of anti-GFP immunoprecipitation, this reverses
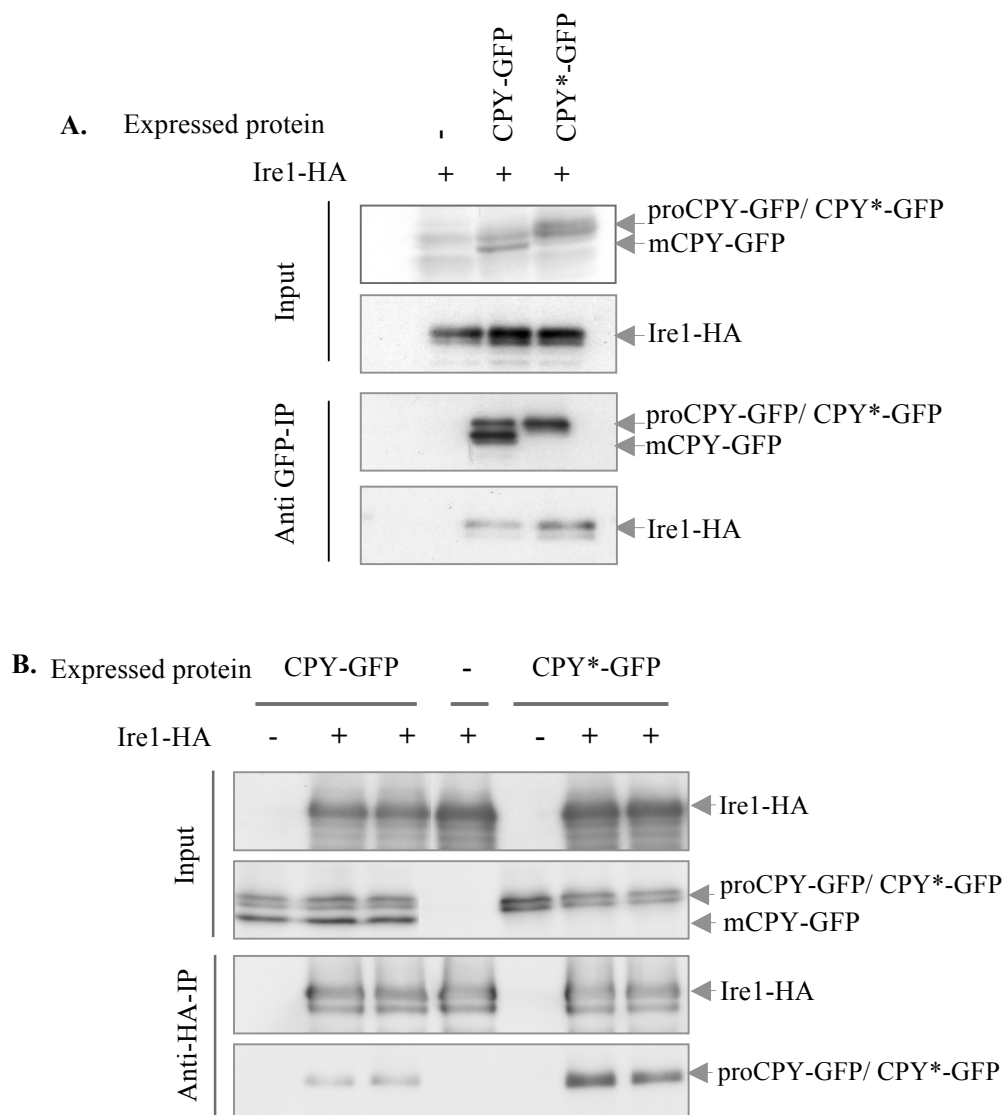
**Figure 10 CPY-GFP and CPY\*-GFP interact with Ire1.** KMY1015 (*ire1Δ*) yeast cells were transformed with pRS426-IRE1-HA together with either pRS313-CPY-GFP or pRS313-CPY\*-GFP or empty vector of pRS313. Cells were then treated with protein crosslinker, DSP. Total cell lysate samples (Input) were subjected to immunoprecipitation (IP) by anti-GFP antibody **(A)** or anti-HA antibody **(B)**. Detection of proteins in the total cell lysates and immunoprecipitates were done by Western blot analyses with anti-HA and anti-GFP antibodies.

immunoprecipitation shows that Ire1-HA association with CPY*-GFP is more obvious than that with wild-type CPY-GFP.

According to the X-ray crystal structure (Credle et al., 2005), the cLD carries a loosely folded segment, namely subregion III (Kimata et al., 2004), which exists as a flexible stretch sticking out from the groove-like structure. To determine whether the groove-like structure actually serves as the binding site of unfolded proteins, two types of yeast Ire1 luminal domain mutants (Fig. 11) were generated. One is Delta-III Ire1, in which subregion III is deleted and thus the groove-like structure may be deformed. The other is the Groove mutant, in which the amino acid residues located on the inner surface of the groove, M229, F285 and Y301, are replaced by alanine.

Yeast cells carrying Groove mutant Ire1 showed severe growth retardation when they were transformed with the plasmid for constitutive expression of CPY*-GFP, probably because the UPR evocation is too weak to cope with accumulation of CPY*-GFP. Therefore, instead of the TEF1 promoter, the galactosidase-inducible GAL1 promoter was used to drive expression of CPY*-GFP.

Anti-GFP immunoprecipitation revealed that wild-type Ire1-HA efficiently co-immunoprecipitated with CPY*-GFP expressed form the GAL1 promoter (Fig. 12). However, the level of Ire1-HA co-immunoprecipitated with CPY*-GFP was decreased by the Delta-III and by the Groove mutations, while anti-HA Western blot analysis of total cell lysates showed that these mutations do not affect the cellular level of Ire1-HA. This finding strongly suggests that the groove-like structure of the Ire1 luminal domain actually functions to capture CPY*-GFP.

In order to address significance of unfolded-protein binding to Ire1, I checked activation of the Ire1 mutants by cellular expression of CPY*-GFP. The β-galactosidase reporter driven by the UPRE showed that expression of CPY*-GFP from the GAL1 promoter through culturing cells in the galactose medium activated wild-type Ire1, but poorly Delta-III Ire1 and Groove mutant Ire1 (Fig. 13). This finding strongly suggests that activation of Ire1 depends on its association with unfolded protein. It also should be noted that activity of Groove mutant Ire1 was weaker than that of Delta-III Ire1 even when cells did not express CPY*-GFP.
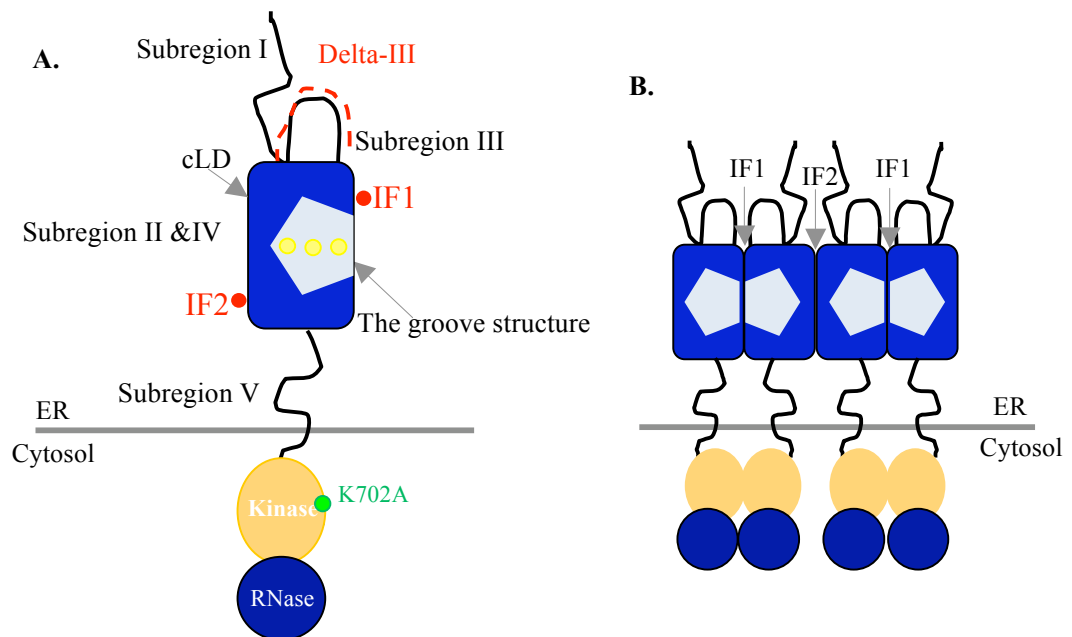
**Figure 11 Structure and mutations of yeast Ire1. (A)** Structure of the monomeric form of Ire1 which is predicated by Kimata et al. (2007) from deletion analysis (Kimata et al., 2004; Oikawa et al., 2005) and X-ray crystallography (Credle et al., 2005). The dashed line indicates the position of deletion in the **Delta-III** mutation (aa 253-272). The red dots indicate the positions of the interface 1 (**IF1**) and the interface 2 (**IF2**) mutations. The yellow dots represent M229, F285 and Y301, which are replaced by alanine in the **Groove mutant**. The green dot indicates the position of the kinase mutant, K702A. **(B)** Homo-association of Ire1 via interfaces 1 and 2 leads to its high-order oligomerization.
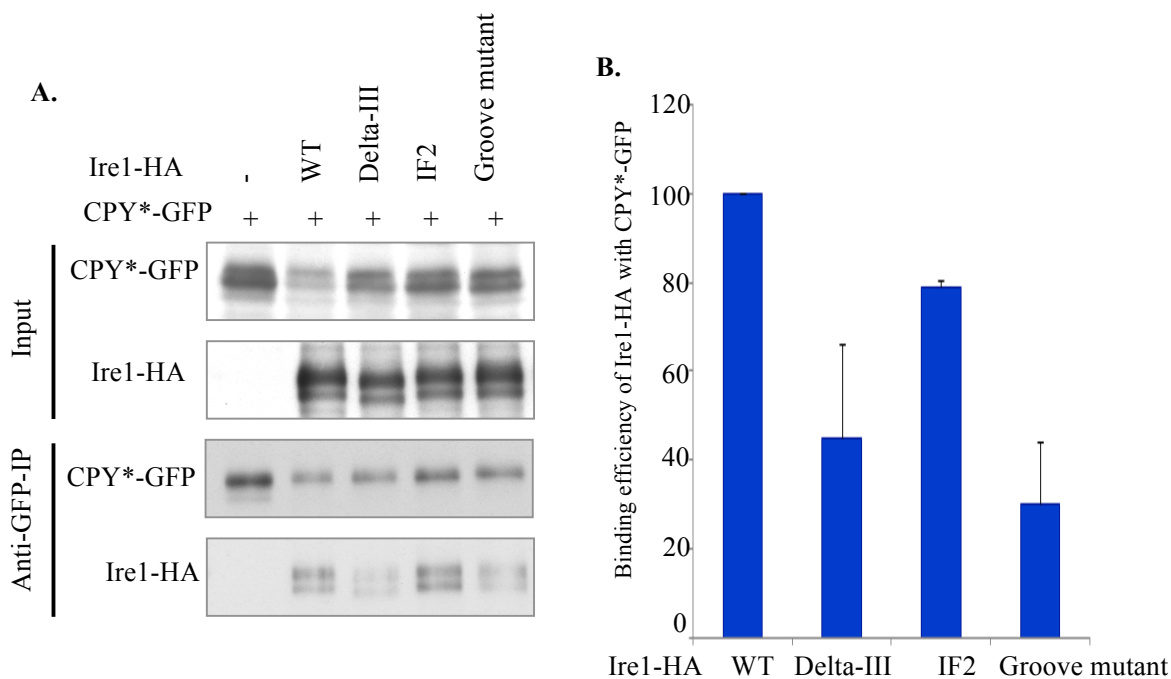
**Figure 12 Interaction of Ire1 mutants with CPY\*-GFP.** Through 14 h culturing in the presence of 2% galactose, CPY\*-GFP was expressed form the GAL1 promoter on plasmid pRS313 in KMY1015 (*ire1Δ*) yeast strain carrying wild-type (WT) or mutant version of pRS426-IRE1-HA. Total cell lysate samples (Input) were then used for anti-GFP immunoprecipitation (IP), products of which were analyzed by Western blotting in (**A**). In (**B**), Ire1-HA signal versus CPY\*-GFP signal for each anti-GFP IP product in (**A**) was quantified and normalized against that of the WT Ire1-HA sample (set at 100), the value of which is expressed as the mean and the standard deviation from three independent clones.
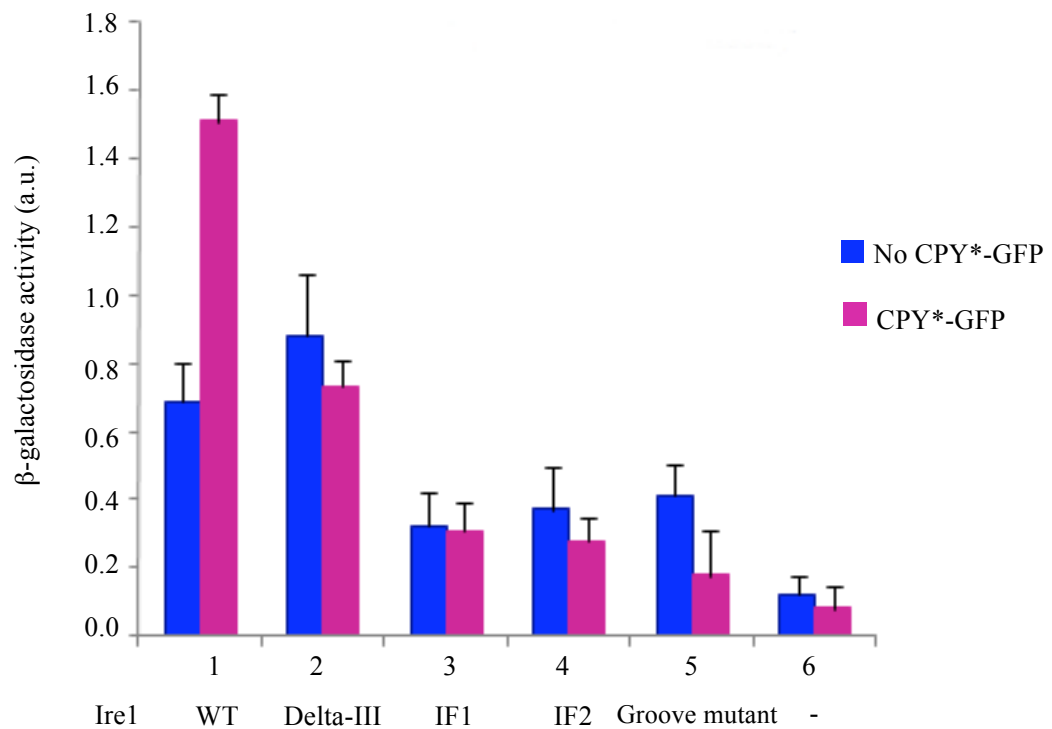
**Figure 13 Acitvation of Ire1 mutants by CPY\*-GFP.** A pRS313-based plasmid for CPY\*-GFP expression from the GAL1 promoter (or empty vector pRS313 for the "no CPY\*-GFP" samples) was co-introduced with either wild-type or mutant version of pRS315-IRE1-HA into the KMY1015 (*ire1Δ*) yeast stain carrying the UPRE-*LacZ* reporter. Cells were then cultured in the presence of 2% galactose for 14 h and checked for cellular β-galactosidase activity.

This implies that as described below, the Groove mutation may confer an unexpected negative effect other than impairment of the unfolded protein association on Ire1 activation.

**3.3 High-order oligomerization and unfolded protein association of Ire1 are likely to be independent events**

As illustrated in Fig. 11, under ER stress condition, Ire1 forms high-order oligomer, (Aragon et al., 2009; Kimata et al., 2007) which is experimentally observed as its dot-like localization through immunofluorescent staining of yeast cells.

In order to approach the causal relationship between the high-order oligomerization and association of the unfolded protein with Ire1, I then employed the IF1 and IF2 mutations, which are deduced to impair homo-association of Ire1 respectively via interfaces 1 and 2 (Fig. 11) (Credle et al., 2005). As shown in Fig. 12, the IF2 mutation only slightly compromised the ability of Ire1 to associate with CPY*-GFP. It should be noted that however, IF2 Ire1 was hardly activated by CPY*-GFP (Fig. 13). For an unknown reason, I failed to obtain reproducible data as for association between IF1 Ire1 and CPY*-GFP.

Even in the case of wild-type Ire1, it is impossible to observe its high-order oligomerization caused by cellular expression of CPY*-GFP (data not shown), probably because this stress is not strong enough. I thus stressed cells by their exposure to a potent ER stressor tunicamycin, which inhibits N-glycosylation of proteins traversing the ER. In Fig. 14, cells expressing Ire1-HA or its mutant versions were stained by anti-HA antibody, reproducing previous observations (Aragon et al., 2009; Kimata et al., 2007). In the absence of stressors, all Ire1-HA variants exhibited a typical ER staining pattern, indicating their diffuse distribution over the ER. Tunicamycin stress altered the localization of wild-type Ire1 and Delta-III Ire1 to a dot-like distribution along the ER, which means those molecules formed high-order oligomer. This finding suggests that the Delta-III mutation specifically compromises
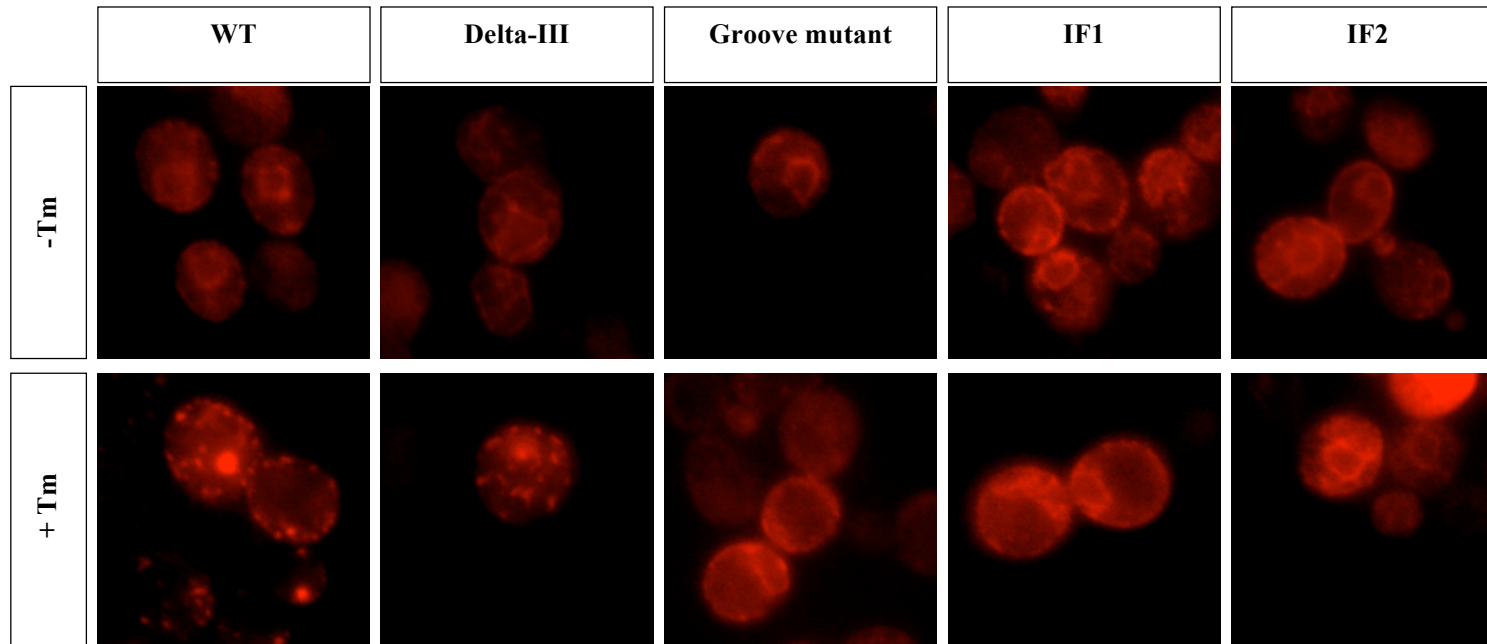
**Figure 14 High-order oligomerization of Ire1 and its luminal domain mutants.** KMY1015 (*ire1Δ*) yeast stain was transformed with wild-type (WT) or mutant versions of pRS426-IRE1-HA. Cells were stressed with 2 μg/ml of tunicamycin for 1 h (+Tm) or remained unstressed (-Tm), and were then stained with anti-HA antibody. The resulting Cy3 signal was observed under a fluorescent microscope.

unfolded proteins associating ability without impairing high-order oligomerization ability of Ire1. Groove mutant Ire1 failed to show the dot-like distribution even under the tunicamycin stress condition. As aforementioned, I think that the Groove mutation somehow causes an unexpected side effect to impair the oligomer formation of Ire1. As expected, IF2 Ire1, as well as IF1 Ire1, also maintained their diffuse staining pattern even under the tunicamycin stress condition.

In Fig. 15, activation of these Ire1 variants by tunicamycin stress was monitored. Although the mutations employed here confer various effects on unfolded-protein association and high-order oligomeization of Ire1, they totally compromised activity of Ire1 to evoke the UPR. Taken together, I propose that high-order oligomerization and interaction of the unfolded-protein with Ire1 are independent events, both of which are required for full activation of Ire1.

## 3.4 Autophosphorylation of Ire1

As noted in the introduction section, activation of Ire1 upon ER stress accompanies its autophosphorylation. I finally addressed the causal relationship between the autophosphorylation and other molecular steps for activation of Ire1. To check the phosphorylation status of Ire1, I added Phos-tag and $Mn^{2+}$ into conventional SDS-PAGE gels to retard migration of phosphorylated proteins (Kinoshita et al., 2006). Since stress by CPY*-GFP expression was too weak to yield a delectable level of phophorylated Ire1 (data not shown), here I also employed tunicamycin stress. In Fig. 16, cell lysates were fractionated by the Phos-tag gels, and Ire1-HA was detected by anti-HA immunoblotting. Dramatically, nearly 100% of wild-type Ire1 proteins were phosphorylated upon cellular treatment of tunicamycin. The mobility shift of Ire1 shown here actually represents the autophosphorylation, since it was not observed when Ire1 carried a kinase mutation K702A. Because Delta-III mutation considerably compromised phosphorylation of Ire1, I think that the unfolded protein interaction contributes to the autophosphorylation.

The IF1 and the IF2 mutations only partially reduced the phosphorylation of Ire1, while Ire1 carrying the double interface mutation of IF1/2 was not phosphorylated at

all. Thus, high-order oligomerization is not likely to be strictly required for autophosphorylation of Ire1. Homo-association only via either interface 1 or 2, dimer formation in other words, of Ire1 can lead to the autophosphorylation, although insufficiently, indicating that both homo-association interfaces are important for Ire1 activity.
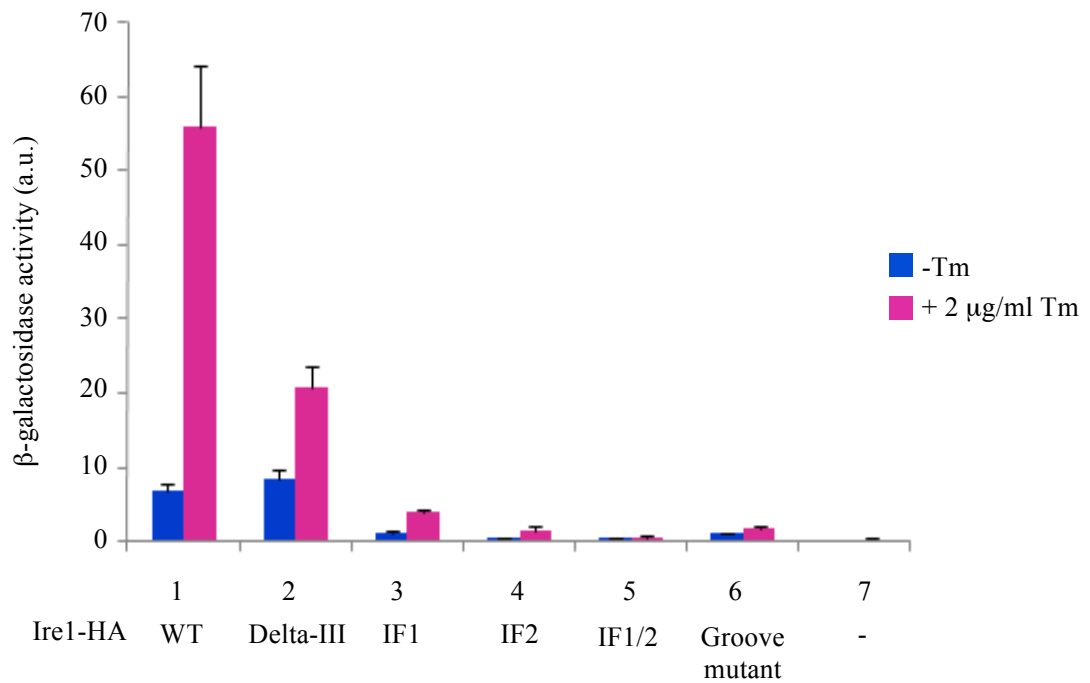
**Figure 15 Activation of Ire1 and its mutants by tunicamycin stress.** Wild-type or mutant versions of pRS315-IRE1-HA was introduced into the KMY1015 yeast strain (*ire1Δ*) carrying the UPRE-*LacZ* reporter. Cells were then treated with or without 2 μg/ml tunicamycin for 4 h, before checking β-galactosidase activity.
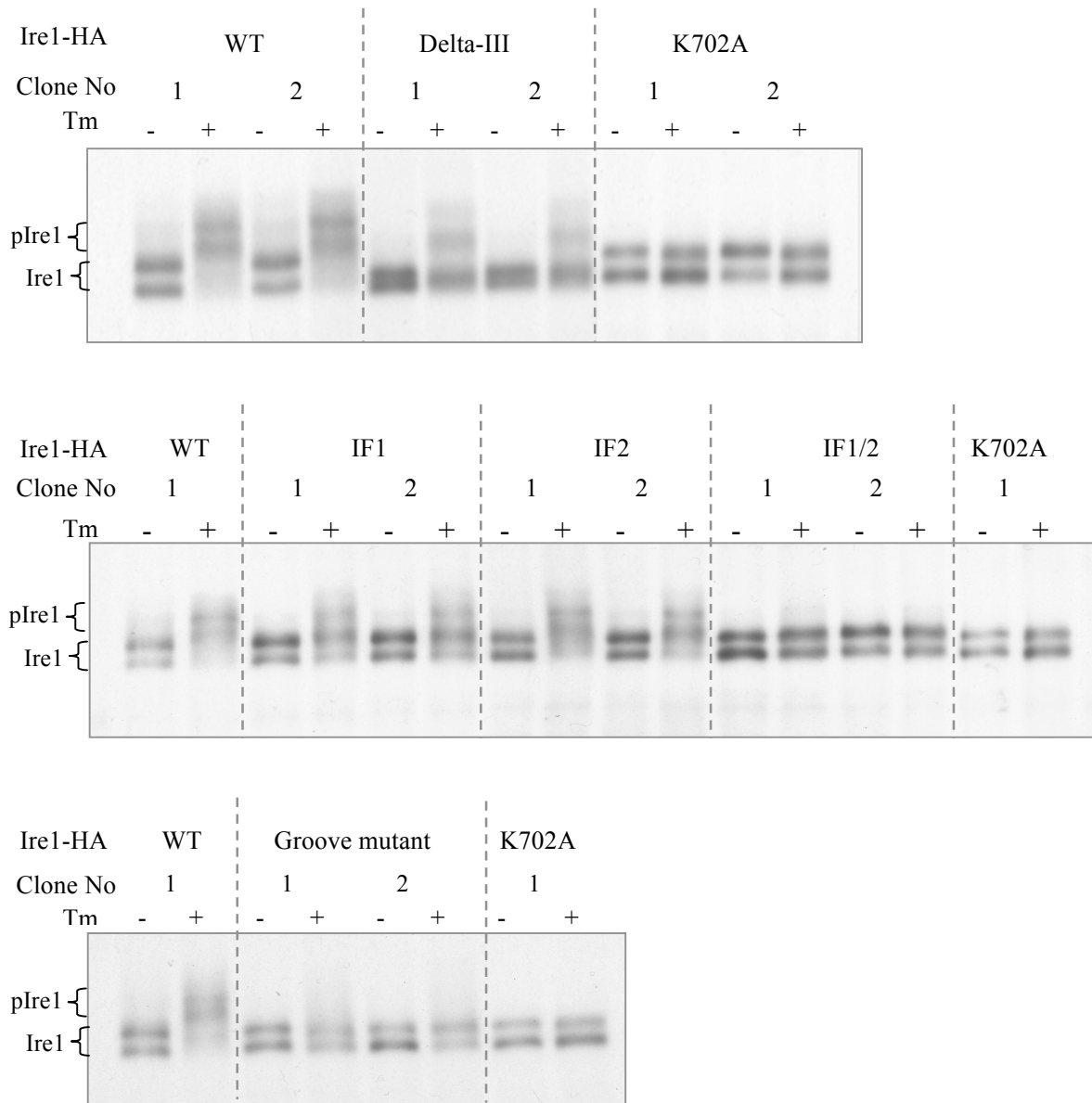
**Figure 16 Auto-phosphorylation of Ire1 and its mutants.** Cells employed in Fig .15 were incubated in the presence or absence of 2 μg/ml tunicamycin for 30 min. Total lysate samples were then prepared in a buffer containing phosphatase and protease inhibitors. 10 μg total proteins were run on SDS-PAGE containing $Mn^{2+}$-Phos-tag and visualized by anti-HA immunoblotting. Ire1 and pIre1 respectively represent unphosphorylated and phosphorylated versions of Ire1.

# CHAPTER IV

# DISCUSSIONS

Kimata et al. (2007) hypothesized that activation of Ire1 by accumulation of unfolded proteins is facilitated via two regulatory steps. First, dissociation of the ER-located molecular chaperone BiP from Ire1 leads to oligomerization of Ire1. Second, direct association of unfolded proteins with the luminal domain of the Ire1 oligomer is required for full activation of Ire1. However, this two-step regulation model is still uncertain because the complexes between Ire1 and unfolded proteins have not been identified. In this study, I have demonstrated that Ire1 interacts with a model unfolded protein *in vivo*. Also, I have addressed how the unfolded protein interaction with Ire1 leads to upregulation of Ire1.

Here I generated an easy-to-detect model of unfolded proteins, CPY*-GFP, which as expected, induces the UPR (Fig. 9) and is accumulated in the ER (Figs. 7 and 8) when expressed in yeast cells. As shown in Fig. 10, I successfully demonstrated the *in vivo* interaction of CPY*-GFP and yeast Ire1. This interaction is biological meaningful for activation of Ire1, because as shown in the case of the Delta-III mutation, impairment of the interaction between Ire1 and CPY*-GFP is likely to be linked to loss of Ire's ability to evoke the UPR (Figs. 12 and 13). Since the Groove mutation also impaired Ire1's ability to interact with unfolded proteins, I think as expected, unfolded proteins are captured by the groove-like structure of the cLD dimer (Fig. 12). According to the X-ray of the cLD, dimer formation via interface 1 but not that via interface 2 is required to form the groove-like structure. This finding is

consistent with my finding that the IF2 mutation only slightly compromised the association between Ire1 and CPY*-GFP (Fig. 12). Therefore, the unfolded-protein association does not require the high-order oligomerization of Ire1, which however, is likely to be a prerequisite for full activation of Ire1 to evoke the UPR (Fig. 13). High-order oligomerization of Ire1 is reported to be required for sterically forming RNA-trapping structure (Korennykh et al., 2009) and gathering the *HAC1* mRNA (Aragon et al., 2009). Taken together, I think that the high-order oligomerization and the unfolded protein association with Ire1 are independent events, although both are required for full evocation of the UPR.

Autophosphorylation of Ire1 has been believed to be an essential step for its activation as an RNase. The autophosphorylation occurs in trans, as one Ire1 molecule phosphorylates a neighboring Ire1 molecule (Shamu and Walter, 1996). In this study, I also checked if the Ire1 luminal domain mutations affect this cytosolic event, and noticed that the Delta-III mutation compromised phosphorylation of Ire1 upon ER stress (Fig. 16). However, it also should be noted as shown in a previous report (Kimata et al., 2007) and in this study (Fig. 14), Delta-III Ire1 exhibits wild-type-like high-order oligomerization in response to ER stress. This observation strongly suggests that the interaction of Ire1 with unfolded proteins does not affect oligomerization status of Ire1 but evokes conformational change of its cytosolic domain, which leads to its autophosporylation and activation as an RNase. In other words, here I propose that the luminal domain communicates stress signal to the cytosolic effector domain by two manners. One is promotion of high-order oligomerization, and the other is a conformational change caused by the direct

interaction of undolded proteins with the cLD. This story resembles the case of some cytokine receptor, which upon binding of ligands, performs not only self-association but also conformational change, causing alteration of cytosolic-domain orientation (Livnah et al., 1999; Remy et al., 1999). I thus believed that binding of unfolded protein with the cLD may be link to conformational change of the cytosolic domain by altering the orientation of the transmembrane domain. This idea is supported by a previous report that the compromised activity of Ire1 by the Delta-III mutation is rescued by a partial deletion of its transmembrane domain (Kimata et al., 2007).

Although Ire1 is evolutionary conserved from yeast to higher eukaryotes, the evolutional homology of the luminal domain is rather low (around 30% identity of the amino-acid sequences). Therefore, the luminal domains of Ire1 orthologues may not play the same role. Mammals carry two Ire1 paralogues, among which Ire1α is a major version expressed ubiquitously. According to the X-ray crystal structure of Ire1α's cLD (Zhou et al., 2006), the size of its groove-like structure is too narrow to associate with unfolded proteins. Also, its orientation in the ER lumen seemed to be inappropriate for capturing unfolded proteins. The idea that Ire1α's cLD cannot be associated with unfolded proteins was supported by Oikawa et al. (2009), (Oikawa et al., 2009) which showed that a recombinant fragment of Ire1α's cLD is not able to inhibit *in vitro* aggregation of unfolded proteins. Since an Ire1α mutant not carrying the major BiP-association subregion was considerably activated even without external ER stress, Oikawa et al. proposed that Ire1α may be mainly regulated only by its association and dissociation from BiP. During the evolution, Ire1α may have lost its ability to directly sense unfolded proteins. Considering difference of the natural

conditions where yeast and mammalian cells live in, I think that it is not strange that an evolutionally conserved sensor protein is regulated in different manners.

The fidelity of response of Ire1, which means Ire1 respond only to ER stress, is an important issue. Chronic and high activation of the UPR are harmful cell, probably because cells have to employ a lot of energy to synthesis UPR responsive-gene products. Indeed, Kawahara et al. (1997) reported that constitutive overexpression of the mature Hac1 protein causes severe growth retardation of yeast cells. In addition, prolonged activation of the UPR pathway is known to trigger program cell death in mammals. In yeast, I think that activation of Ire1 is tightly regulated by the two-step regulatory mechanisms which I touch on in this study. Meanwhile, in the case of mammalian cells, Ire1α is known to be regulated by various associating proteins, which may be responsible for appropriate regulation of Ire1α (Kimata and Kohno, 2011).

# ACKNOWLEDGEMENTS

Thanyarat Promlek

# REFERENCES

Aragon, T., van Anken, E., Pincus, D., Serafimova, I.M., Korennykh, A.V., Rubio, C.A., and Walter, P. (2009). Messenger RNA targeting to endoplasmic reticulum stress signalling sites. Nature *457*, 736-740.

Bernales, S., Papa, F.R., and Walter, P. (2006). Intracellular signaling by the unfolded protein response. Annu Rev Cell Dev Biol *22*, 487-508.

Calfon, M., Zeng, H., Urano, F., Till, J.H., Hubbard, S.R., Harding, H.P., Clark, S.G., and Ron, D. (2002). IRE1 couples endoplasmic reticulum load to secretory capacity by processing the XBP-1 mRNA. Nature *415*, 92-96.

Cox, J.S., Shamu, C.E., and Walter, P. (1993). Transcriptional induction of genes encoding endoplasmic reticulum resident proteins requires a transmembrane protein kinase. Cell *73*, 1197-1206.

Cox, J.S., and Walter, P. (1996). A novel mechanism for regulating activity of a transcription factor that controls the unfolded protein response. Cell *87*, 391-404.

Credle, J.J., Finer-Moore, J.S., Papa, F.R., Stroud, R.M., and Walter, P. (2005). On the mechanism of sensing unfolded protein in the endoplasmic reticulum. Proc Natl Acad Sci U S A *102*, 18773-18784.

Finger, A., Knop, M., and Wolf, D.H. (1993). Analysis of two mutated vacuolar proteins reveals a degradation pathway in the endoplasmic reticulum or a related compartment of yeast. Eur J Biochem *218*, 565-574.

Harding, H.P., Novoa, I., Zhang, Y., Zeng, H., Wek, R., Schapira, M., and Ron, D. (2000). Regulated translation initiation controls stress-induced gene expression in mammalian cells. Mol Cell *6*, 1099-1108.

Hetz, C., and Glimcher, L.H. (2009). Fine-tuning of the unfolded protein response: Assembling the IRE1alpha interactome. Mol Cell *35*, 551-561.

Humpolickova, J., Benda, A., and Enderlein, J. (2009). Optical saturation as a versatile tool to enhance resolution in confocal microscopy. Biophys J *97*, 2623-2629.

Jung, G., Ueno, H., and Hayashi, R. (1999). Carboxypeptidase Y: structural basis for protein sorting and catalytic triad. J Biochem *126*, 1-6.

Kawahara, T., Yanagi, H., Yura, T., and Mori, K. (1997). Endoplasmic reticulum stress-induced mRNA splicing permits synthesis of transcription factor Hac1p/Ern4p that activates the unfolded protein response. Mol Biol Cell *8*, 1845-1862.

Kimata, Y., Ishiwata-Kimata, Y., Ito, T., Hirata, A., Suzuki, T., Oikawa, D., Takeuchi, M., and Kohno, K. (2007). Two regulatory steps of ER-stress sensor Ire1 involving its cluster formation and interaction with unfolded proteins. J Cell Biol *179*, 75-86.

Kimata, Y., Kimata, Y.I., Shimizu, Y., Abe, H., Farcasanu, I.C., Takeuchi, M., Rose, M.D., and Kohno, K. (2003). Genetic evidence for a role of BiP/Kar2 that regulates Ire1 in response to accumulation of unfolded proteins. Mol Biol Cell *14*, 2559-2569.

Kimata, Y., and Kohno, K. (2011). Endoplasmic reticulum stress-sensing mechanisms in yeast and mammalian cells. Curr Opin Cell Biol *23*, 135-142.

Kimata, Y., Oikawa, D., Shimizu, Y., Ishiwata-Kimata, Y., and Kohno, K. (2004). A role for BiP as an adjustor for the endoplasmic reticulum stress-sensing protein Ire1. J Cell Biol *167*, 445-456.

Kinoshita, E., Kinoshita-Kikuta, E., Takiyama, K., and Koike, T. (2006). Phosphate-binding tag, a new tool to visualize phosphorylated proteins. Mol Cell Proteomics *5*, 749-757.

Kohno, K., Normington, K., Sambrook, J., Gething, M.J., and Mori, K. (1993). The promoter region of the yeast KAR2 (BiP) gene contains a regulatory domain that

responds to the presence of unfolded proteins in the endoplasmic reticulum. Mol Cell Biol *13*, 877-890.

Livnah, O., Stura, E.A., Middleton, S.A., Johnson, D.L., Jolliffe, L.K., and Wilson, I.A. (1999). Crystallographic evidence for preformed dimers of erythropoietin receptor before ligand activation. Science *283*, 987-990.

Ma, Y., and Hendershot, L.M. (2004). The role of the unfolded protein response in tumour development: friend or foe? Nat Rev Cancer *4*, 966-977.

Malhotra, J.D., and Kaufman, R.J. (2007). The endoplasmic reticulum and the unfolded protein response. Semin Cell Dev Biol *18*, 716-731.

Mori, K., Kawahara, T., Yoshida, H., Yanagi, H., and Yura, T. (1996). Signalling from endoplasmic reticulum to nucleus: transcription factor with a basic-leucine zipper motif is required for the unfolded protein-response pathway. Genes Cells *1*, 803-817.

Mori, K., Ogawa, N., Kawahara, T., Yanagi, H., and Yura, T. (2000). mRNA splicing-mediated C-terminal replacement of transcription factor Hac1p is required for efficient activation of the unfolded protein response. Proc Natl Acad Sci U S A *97*, 4660-4665.

Mori, K., Sant, A., Kohno, K., Normington, K., Gething, M.J., and Sambrook, J.F. (1992). A 22 bp cis-acting element is necessary and sufficient for the induction of the yeast KAR2 (BiP) gene by unfolded proteins. EMBO J *11*, 2583-2593.

Oikawa, D., Kimata, Y., and Kohno, K. (2007). Self-association and BiP dissociation are not sufficient for activation of the ER stress sensor Ire1. J Cell Sci *120*, 1681-1688.

Oikawa, D., Kimata, Y., Kohno, K., and Iwawaki, T. (2009). Activation of mammalian IRE1alpha upon ER stress depends on dissociation of BiP rather than on direct interaction with unfolded proteins. Exp Cell Res *315*, 2496-2504.

Oikawa, D., Kimata, Y., Takeuchi, M., and Kohno, K. (2005). An essential dimer-forming subregion of the endoplasmic reticulum stress sensor Ire1. Biochem J *391*, 135-142.

Okamura, K., Kimata, Y., Higashio, H., Tsuru, A., and Kohno, K. (2000). Dissociation of Kar2p/BiP from an ER sensory molecule, Ire1p, triggers the unfolded protein response in yeast. Biochem Biophys Res Commun *279*, 445-450.

Remy, I., Wilson, I.A., and Michnick, S.W. (1999). Erythropoietin receptor activation by a ligand-induced conformation change. Science *283*, 990-993.

Ron, D., and Walter, P. (2007). Signal integration in the endoplasmic reticulum unfolded protein response. Nat Rev Mol Cell Biol *8*, 519-529.

Shamu, C.E., and Walter, P. (1996). Oligomerization and phosphorylation of the Ire1p kinase during intracellular signaling from the endoplasmic reticulum to the nucleus. EMBO J *15*, 3028-3039.

Sidrauski, C., Cox, J.S., and Walter, P. (1996). tRNA ligase is required for regulated mRNA splicing in the unfolded protein response. Cell *87*, 405-413.

Sidrauski, C., and Walter, P. (1997). The transmembrane kinase Ire1p is a site-specific endonuclease that initiates mRNA splicing in the unfolded protein response. Cell *90*, 1031-1039.

Spear, E.D., and Ng, D.T. (2003). Stress tolerance of misfolded carboxypeptidase Y requires maintenance of protein trafficking and degradative pathways. Mol Biol Cell *14*, 2756-2767.

Tirasophon, W., Lee, K., Callaghan, B., Welihinda, A., and Kaufman, R.J. (2000). The endoribonuclease activity of mammalian IRE1 autoregulates its mRNA and is required for the unfolded protein response. Genes Dev *14*, 2725-2736.

Tirasophon, W., Welihinda, A.A., and Kaufman, R.J. (1998). A stress response pathway from the endoplasmic reticulum to the nucleus requires a novel bifunctional protein kinase/endoribonuclease (Ire1p) in mammalian cells. Genes Dev *12*, 1812-1824.

Yoshida, H., Haze, K., Yanagi, H., Yura, T., and Mori, K. (1998). Identification of the cis-acting endoplasmic reticulum stress response element responsible for transcriptional induction of mammalian glucose-regulated proteins. Involvement of basic leucine zipper transcription factors. J Biol Chem *273*, 33741-33749.

Yoshida, H., Oku, M., Suzuki, M., and Mori, K. (2006). pXBP1(U) encoded in XBP1 pre-mRNA negatively regulates unfolded protein response activator pXBP1(S) in mammalian ER stress response. J Cell Biol *172*, 565-575.

# 論　文　目　録

| 所　属<br>(主指導教員) | 動物細胞工学研究室<br>(河野　憲二) | | |
|---|---|---|---|
| 氏　名 | Promlek Thanyarat | 提　出 | 平成 23年　8月　11 日 |

学位論文の主たる部分を公表した論文
（題名、全著者名、公表時期、雑誌名、巻、ページ）


Membrane aberrancy and unfolded proteins activate the endoplasmic reticulum-stress sensor Ire1 by different manners.

Thanyarat Promlek, Yuki Ishiwata-Kimata, Masahiro Shido, Mitsuru Sakuramoto, Kenji Kohno and Yukio Kimata

参考論文
（題名、全著者名、公表時期、雑誌名、巻、ページ）